Available online at www.sciencedirect.com

ScienceDirect

Procedia Structural Integrity 25 (2020) 355–363

Structural Integrity Procedia

www.elsevier.com/locate/procedia

1st Virtual Conference on Structural Integrity - VCSI1

Evaluation of fatigue properties of 3D-printed Polyamide-12 by means of energy approach during tensile tests

Dario Santonocito*

University of Messina, Department of Engineering, Contrada di Dio, 98166 Messina, Italy

Abstract

Rapid prototyping and Additive Manufacturing are experiencing a continuous and rapid growth in different industrial fields, ranging from automotive to biomedical applications. They allow the creation of a wide range of devices in a short time with several materials, such as polymers and metals. On the other hand, the manufacturing process considerably affects the performance of the obtained 3D-printed materials and different laboratory tests are required in order to assess the mechanical properties, especially the fatigue behavior, of these materials.
The present work is the result of the collaboration between the Engineering Department of the University of Messina and the rapid-prototyping company Skorpion Engineering. The aim of this work is to apply, for the first time on 3D-printed materials, the Static Thermographic Method for the fatigue assessment of Polyamide-12.

Keywords: fatigue assessment; Multijet Fusion; Static Thermographic Method; additive manufacturing.

1. Introduction

Additive Manufacturing (AM) is spreading in several industrial fields (Ngo et al., 2018) such as automotive (Schmitt et al., 2019), aerospace and aeronautics (Singamneni et al., 2019) and biomedical (Coulter et al., 2019; Revilla-León and Özcan, 2019). Combined with topology optimization it allows the creation of many devices with a

* Corresponding author. Tel.: +39 3396190552.
E-mail address: dsantonocito@unime.it

10.1016/j.prostr.2020.04.040

variety of shape and functional design unattainable through traditional mechanical process (Cucinotta et al., 2020, 2019; Dapogny et al., 2019). Rapid prototyping enables the creation of final products directly from the CAD file, requiring design strategy in order to avoid the physical testing, adopting advanced simulation, structural optimization and failure prevention methods (Berto et al., 2018). On the other hand, AM materials presents several issues due to the uncertainty of their mechanical performances. Many authors have investigated the mechanical properties of AM materials, both polymers (O'Connor et al., 2018; Stoia et al., 2019) and metals (Meneghetti et al., 2019; Razavi et al., 2018). Especially the fatigue properties require a huge amount of time and a large number of specimens in order to be assessed, hence the infrared thermography (IR) could be a valid aid in the investigation of these properties. It has been applied on different materials subjected to several loading conditions: notched and plain steel specimens under static and fatigue tests (Ricotta et al., 2019; Rigon et al., 2019; Risitano and Risitano, 2013), laminated composites under tensile static loading (Vergani et al., 2014), polyethylene under static and fatigue loading (Risitano et al., 2018), short glass fiber-reinforced polyamide composites under static and fatigue loading (V. Crupi et al., 2015), steels under high cycle (Amiri and Khonsari, 2010; Corigliano et al., 2019; Curà et al., 2005; Meneghetti et al., 2013) and very high cycle fatigue regimes (V Crupi et al., 2015; Plekhov et al., 2015). In 2000, La Rosa and Risitano, proposed the Thermographic Method (TM) as an innovative approach based on thermographic analyses of the temperature evolution during the fatigue tests in order to predict the fatigue limit and the S-N curve (Fargione et al., 2002). In 2013, Risitano and Risitano proposed the Static Thermographic Method (STM) as a rapid procedure to derive the fatigue limit of the material evaluating the temperature evolution during a static tensile test.

The aim of this research activity is the application of the STM during static tensile tests for the first time on a 3D-printed plastic material. Tensile tests were carried out and IR thermography has been adopted during all the static tests in order to evaluate the energetic release of the material. This research activity is part of the collaboration between the University of Messina and the rapid-prototyping company Skorpion Engineering.

Nomenclature

c	specific heat capacity of the material [J/kg.K]
E	Young's Modulus [MPa]
K_m	thermoelastic coefficient [MPa^{-1}]
R	stress ratio
t	test time [s]
T, T_i	instantaneous value of temperature [K]
T_0	initial value of temperature estimated at time zero [K]
v	displacement velocity [mm/min]
α	thermal diffusivity of the material [m^2/s]
ΔT_s	absolute surface temperature variation during a static tensile test [K]
ΔT_1	estimated value of temperature for the first set of temperature data [K]
ΔT_2	estimated value of temperature for the second set of temperature data [K]
ε, ε_f	strain, strain at failure
ε_1, ε_2	strain level for elastic modulus linear regression
ρ	density of the material [kg/m^3]
σ, σ_1	stress level, uniaxial stress [MPa]
σ_D	critical macro stress that produces irreversible micro-plasticity [MPa]
σ_{lim}	fatigue limit estimated with the Static Thermographic Method [MPa]
σ_U	ultimate tensile strength [MPa]

2. Theoretical Background

During a uniaxial traction test of common engineering materials, the temperature evolution, detected by means of an infrared camera, is characterized by three phases (Fig. 1): an initial approximately linear decrease due to the

thermoelastic effect (Phase I), then the temperature deviates from linearity until a minimum (Phase II) and a very high further temperature increment until failure (Phase III).

In adiabatic conditions and for linear isotropic homogeneous material, the variation of the material temperature under uniaxial stress state follows the Lord Kelvin's law:

$$\Delta T_s = -\frac{\alpha}{\rho \cdot c} T \sigma_1 = -K_m T \sigma_1 \tag{1}$$

where K_m is the thermoelastic coefficient.

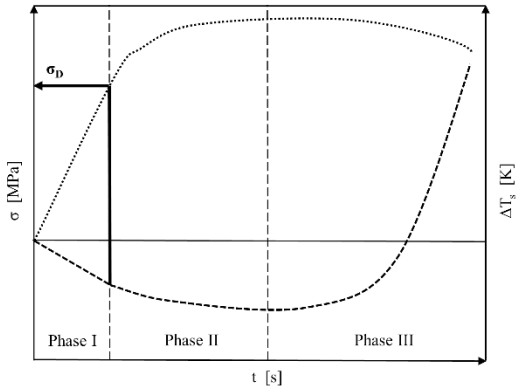

Fig. 1. Temperature trend vs. load during a static traction test.

The use of high precision IR sensors allows to define experimental temperature vs. time diagram during static tensile test in order to define the stress at which the linearity is lost. Clienti et al. (2010) for the first time correlated the damage stress σ_D related to the first deviation from linearity of ΔT temperature increment during static test (end of Phase I) to the fatigue limit of plastic materials. Risitano and Risitano (2013) proposed a novel procedure to assess the fatigue limit of the materials during monoaxial tensile test. If it is possible during a static test to estimate the stress at which the temperature trend deviates from linearity, that stress could be related to a critical macro stress σ_D which is able to produce in the material irreversible micro-plasticity. This critical stress is the same stress that, if cyclically applied to the material, will increase the microplastic area up to produce microcracks, hence fatigue failure.

3. Materials and methods

Static tensile test were performed on specimen made of 3D-printed Polyamide-12, according to the geometry prescribed by the ASTM D638 standard, with a nominal cross section of 13 mm x 7 mm (Fig. 2a). The specimens were realised with a HP Jet Fusion 3D 4200 printer, along the XY plane, adopting the polymeric powder HP 3D High Reusability PA12, with a powder melting point (DSC) of 187°C, particle size of 60 µm and bulk density 0.425 g/cm^3. The printer adopts the Multijet Fusion (MJF™) printing system: it is a powder-based technology without the adoption of a laser source. The powder bed is preheated uniformly and a first layer of liquid fusion agents is deposited on the printing plane, later a second layer with detailing agents is deposited in the points where the material need to be melted. A source of infrared energy, usually planar lamps, pass over the surface of the bed allowing the powder fusion. The process continues, layer by layer, up to the completion of the component. The specimens were printed adopting the "Fast" printing profile, which ensure a rapid printing process, but with lower mechanical properties compared to the "Mechanical" profile.

The tests were performed with a servo-hydraulic load machine ITALSIGMA 25 kN with a crosshead rate equal to 5 mm/min, at constant temperature and relative humidity (23°C and 50% RH) (Fig. 2b). The tensile tests were carried out on three specimens and an infrared camera FLIR A40, with a sample rate of 1 image per second, was adopted to monitoring the specimen's surface temperature. Longitudinal displacements of the specimen were

assessed by means of a Digital Image Correlation system GOM Aramis 3D 12M. The specimen surfaces were coated with high emissivity black paint on one side while with a speckle pattern on the other side.

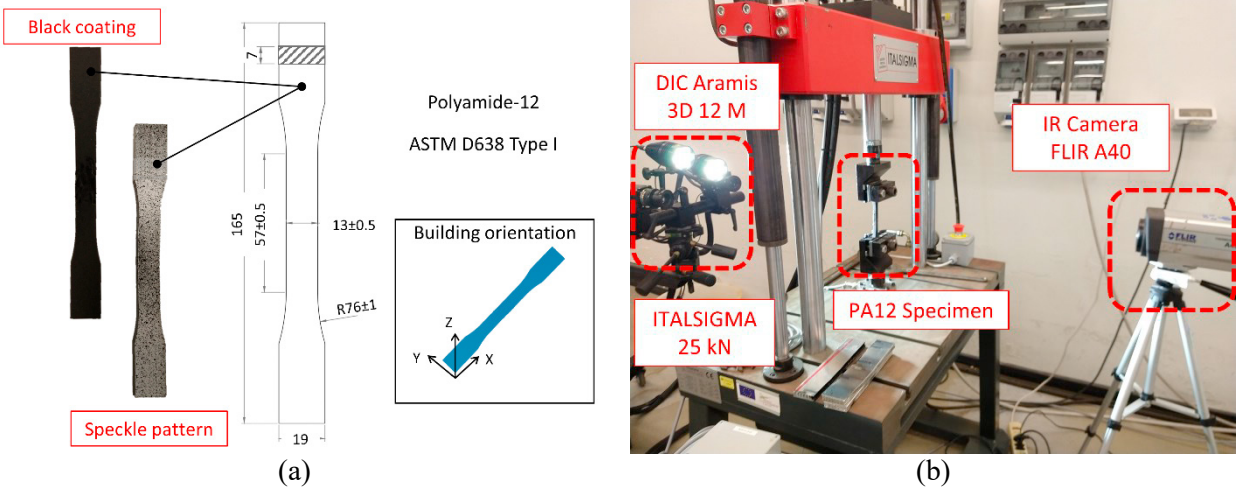

Fig. 2. a) Specimen geometry and building characteristics; b) experimental setup.

A series of fatigue tests at constant amplitude was performed on seven specimens of the same geometry of the previous ones, with a stress ratio R= 0.1 and a test frequency f= 3 Hz. After the tests, the fracture surfaces of the specimens were analysed adopting a high definition optical microscope LEICA.

4. Results and discussion

4.1 Mechanical properties

Static traction tests were performed on three specimens under displacement control, with a velocity of 5 mm/min. The DIC was adopted in order to assess the local displacement on the specimens while the IR camera was adopted to monitor the superficial temperature evolution. In Fig. 3 are reported the engineering curves for the three tested specimens. The stress is evaluated as the ratio between the force and the nominal cross section area of the specimen, while the strain as the ratio of the distance variation of two spot over their initial distance (L_0= 10 mm). The Young's Modulus has been evaluated as the linear regression of the stress vs strain between ε_1=0.0005 and ε_2=0.0025.

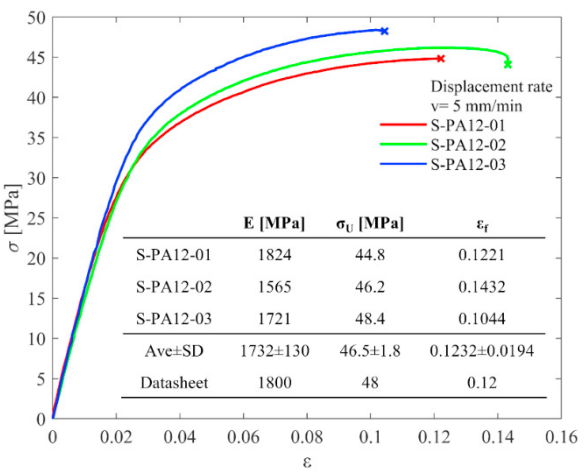

	E [MPa]	σ_U [MPa]	ε_f
S-PA12-01	1824	44.8	0.1221
S-PA12-02	1565	46.2	0.1432
S-PA12-03	1721	48.4	0.1044
Ave±SD	1732±130	46.5±1.8	0.1232±0.0194
Datasheet	1800	48	0.12

Fig. 3. Engineering curve and mechanical properties for PA12

As observed by Stoia et al. (2019) for SLS 3D-printed PA2200, this kind of material exhibit a linear elastic behavior followed by a smooth hardening until failure, and, in addition, it is not possible to assess a yield point. Considering the values of the mechanical properties for PA12 Type I specimens printed with "Fast" profile along XY direction, as reported by the manufacturer datasheet, it is possible to note how they fall within the range of the average and one standard deviation for the three tests. The mechanical properties are also in agreement with the ones found by Lammens et al. (2017) for Selective Laser Sintering PA12 specimens, tested at 5 mm/min. For PA12 specimens obtained by MJF™ system, O'Connor et al. (2018) found lower values of the elastic modulus (E= ~1240 MPa) and higher elongation at break (ε_f= ~0.19), while Morales-Planas et al. (2018) a lower elongation at break (ε_f= ~0.05).

4.2 Static Thermographic Method and fatigue limit

During static tensile tests, the evolution of the specimen's surface temperature has been evaluated by means of an IR camera. The applied stress is reported versus the specimen's surface temperature variation, estimated as the difference between the instantaneous temperature and the initial temperature of the surface recorded at time zero ($\Delta T = T_i - T_0$) (Fig. 4).

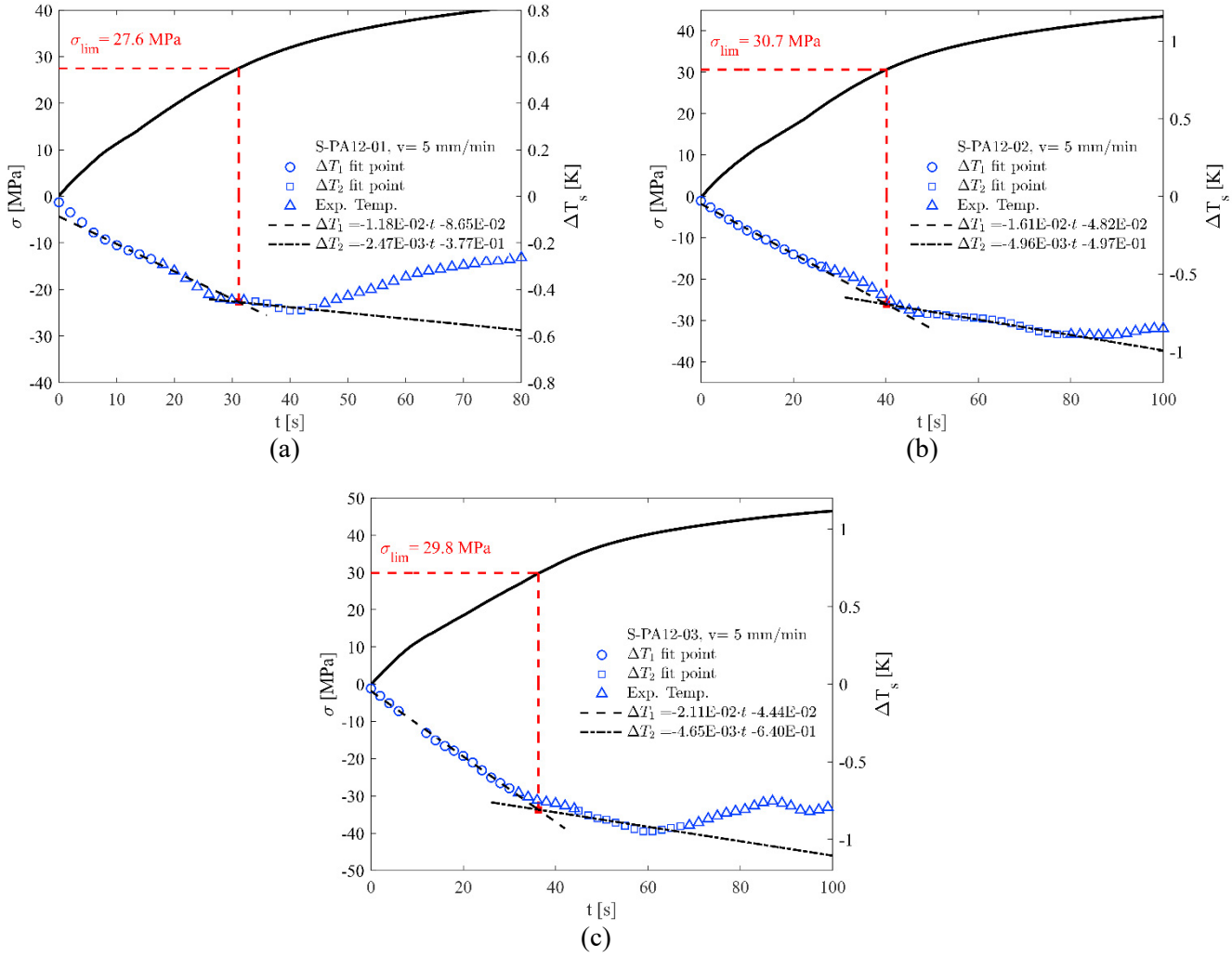

Fig. 4. Temperature evolution vs. applied stress during static tensile test on PA12 specimens.

The temperature data has been filtered with a *rlowess* filter, with a data span of 10%, in order to reduce the outliers and highlight the thermoelastic trend. In the initial part of the ΔT-t curve it is possible to clearly distinguish the linear trend of the temperature, then it deviates from the linearity reaching a plateau region, suddenly it experiences a rapid increment. It is possible to draw two linear regression line, the former for the first linear phase (early stage of the temperature signal, ΔT_1 fit point series) and the latter for the second phase (last stage before the sudden increase in the temperature signal, ΔT_2 fit point series), not taking into account the temperature values near the slope change (Experimental Temperature series). Solving the system of equations, it is possible to determine the intersection point of the two straight lines. The corresponding value of the applied stress, namely σ_{lim}, could be related to the macroscopic stress that introduces the first plasticization phenomena in the material. For the three static tensile tests an average value of 29.4±1.6 MPa has been found for the limit stress.

Useful information can be also retrieved observing the temperature trend. In particular, it is possible to define a yielding stress in correspondence of the temperature zero-derivative flex region, in the transition point between Phase II and Phase III. This stress can be thought as the macroscopic stress at which the majority of the material crystals are under plastic condition.

A series of fatigue tests has been carried out with constant stress amplitude, equal to 28 MPa and 30 MPa. In Fig. 5 are reported in a S-N plot the test results, adopting a number of cycle for run out of $N_A = 2x10^6$. In the same plot are reported the average value and the scatter band with one standard deviation for the limit stress assessed by STM. As is possible to note, both failure and run out tests falls within the scatter band; hence the stress value assessed by means of the STM could be related with the fatigue limit of the material. However, several traditional fatigue tests have to be carried out to obtain the S-N curve and the fatigue limit of the material.

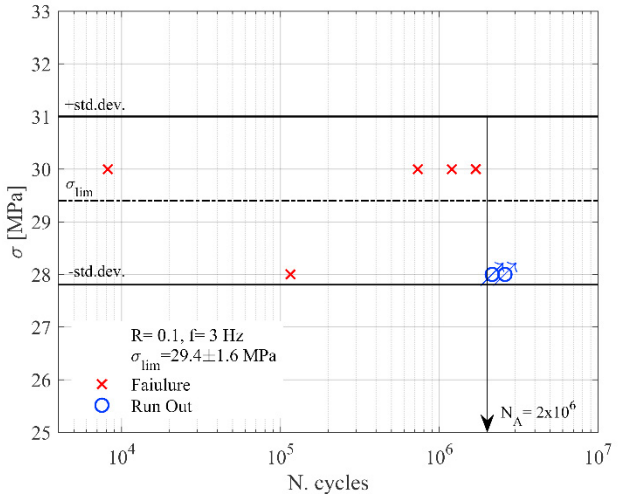

Fig. 5. Comparison between the stress limit and the traditional fatigue tests

4.3 Fracture surfaces

After static and fatigue tests the fracture surfaces have been evaluated through an optical microscope. In Fig. 6, are reported the fracture surfaces of a sample per test typology; the other samples exhibit the same behavior. As regard to the static tests (Fig. 6a), the fracture surfaces show the classical aspect of a ductile failure, with small plastic deformation. In all of the static fracture surfaces are clearly visible a series of defects due to the lack of powder melting. In particular, defects with a diameter of about 1 mm has been found surrounded by non-melted powder where it is possible to distinguish the different layers.

Fatigue fracture surfaces show a smoother profile, typical of a brittle failure (Fig. 6b). The surface appears darker than the static case and this could be addressed to the increase in specimen's temperature due to the fatigue tests frequency (Hülsbusch et al., 2019). Defects due to the lack of powder melting, with an average diameter of 0.3 mm, have been found. Also in this case, the different layers of material could be observed near the circular defects area,

with an average length of the cracks equal to 0.6 mm. From the analysis of the fracture surfaces it is evident how the printing process affects the mechanical properties of the materials both under static and fatigue tests (Wang et al., 2019).

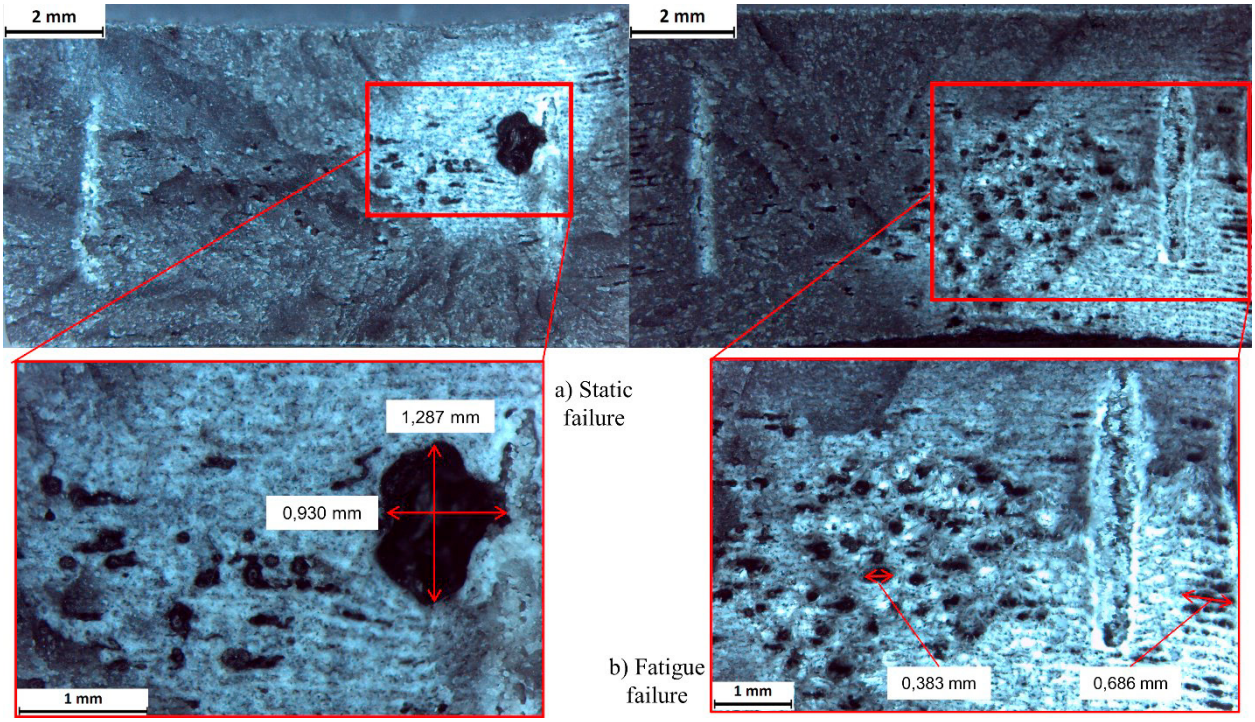

Fig. 6. Fracture surfaces for: a) static tensile tests; b) fatigue tests

5 Conclusion

In this work the energetic release during tensile tests on 3D printed polyamide-12 specimens has been evaluated. The mechanical properties of the material have been assessed and compared to other authors and datasheet values showing good agreement. During the same tensile tests, the IR camera allowed the application of the Static Thermographic Method, monitoring the specimen's surface temperature. The average value of the limit stress has been evaluated as the stress level at which the temperature deviates from its linear trend, obtaining a value of 29.4±1.6 MPa. This value has been compared with traditional fatigue test showing a relation with the fatigue limit of the material. Micrographic analysis of the fracture surfaces have been performed showing how the printing process severally affects the mechanical properties of the material under static and fatigue loading.

The Static Thermographic Method could be adopted in rapid prototyping process as a fast test procedure able to predict the fatigue properties of the 3D-printed materials from a conventional static test in a very short amount of time and with a limited number of specimens.

Acknowledgment

The author would like to thanks Skorpion Engineering S.r.l, for providing all the necessary materials, and Prof. Giacomo Risitano's research group for the support on this research activity.

References

Amiri, M., Khonsari, M.M., 2010. Rapid determination of fatigue failure based on temperature evolution: Fully reversed bending load. Int. J. Fatigue 32, 382–389. https://doi.org/10.1016/j.ijfatigue.2009.07.015

Berto, F., Razavi, S.M.J., Torgersen, J., 2018. Frontiers of fracture and fatigue: Some recent applications of the local strain energy density. Frat. ed Integrita Strutt. 12, 1–32. https://doi.org/10.3221/IGF-ESIS.43.01

Clienti, C., Fargione, G., La Rosa, G., Risitano, A., Risitano, G., 2010. A first approach to the analysis of fatigue parameters by thermal variations in static tests on plastics. Eng. Fract. Mech. 77, 2158–2167. https://doi.org/10.1016/j.engfracmech.2010.04.028

Corigliano, P., Cucinotta, F., Guglielmino, E., Risitano, G., Santonocito, D., 2019. Fatigue assessment of a marine structural steel and comparison with Thermographic Method and Static Thermographic Method. FFEMS 1–10. https://doi.org/10.1111/ffe.13158

Coulter, F.B., Schaffner, M., Faber, J.A., Rafsanjani, A., Smith, R., Appa, H., Zilla, P., Bezuidenhout, D., Studart, A.R., 2019. Bioinspired Heart Valve Prosthesis Made by Silicone Additive Manufacturing. Matter 1, 266–279. https://doi.org/10.1016/j.matt.2019.05.013

Crupi, V, Epasto, G., Guglielmino, E., Risitano, G., 2015. Thermographic method for very high cycle fatigue design in transportation engineering. Proc. Inst. Mech. Eng. Part C J. Mech. Eng. Sci. 229, 1260–1270. https://doi.org/10.1177/0954406214562463

Crupi, V., Guglielmino, E., Risitano, G., Tavilla, F., 2015. Experimental analyses of SFRP material under static and fatigue loading by means of thermographic and DIC techniques. Compos. Part B Eng. 77, 268–277. https://doi.org/10.1016/j.compositesb.2015.03.052

Cucinotta, F., Guglielmino, E., Longo, G., Risitano, G., Santonocito, D., Sfravara, F., 2019. Topology optimization additive manufacturing-oriented for a biomedical application, Lecture Notes in Mechanical Engineering. Springer International Publishing. https://doi.org/10.1007/978-3-030-12346-8_18

Cucinotta, F., Raffaele, M., Salmeri, F., 2020. A Topology Optimization of a Motorsport Safety Device, in: Rizzi, C., Andrisano, A.O., Leali, F., Gherardini, F., Pini, F., Vergnano, A. (Eds.), Design Tools and Methods in Industrial Engineering. Springer International Publishing, Cham, pp. 400–409.

Curà, F., Curti, G., Sesana, R., 2005. A new iteration method for the thermographic determination of fatigue limit in steels. Int. J. Fatigue 27, 453–459. https://doi.org/10.1016/j.ijfatigue.2003.12.009

Dapogny, C., Estevez, R., Faure, A., Michailidis, G., 2019. Shape and topology optimization considering anisotropic features induced by additive manufacturing processes. Comput. Methods Appl. Mech. Eng. 344, 626–665. https://doi.org/10.1016/j.cma.2018.09.036

Fargione, G., Geraci, A., La Rosa, G., Risitano, A., 2002. Rapid determination of the fatigue curve by the thermographic method. Int. J. Fatigue 24, 11–19. https://doi.org/10.1016/S0142-1123(01)00107-4

Hülsbusch, D., Kohl, A., Striemann, P., Niedermeier, M., Walther, F., 2019. Development of an energy-based approach for optimized frequency selection for fatigue testing on polymers – Exemplified on polyamide 6. Polym. Test. 106260. https://doi.org/10.1016/j.polymertesting.2019.106260

La Rosa, G., Risitano, A., 2000. Thermographic methodology for rapid determination of the fatigue limit of materials and mechanical components. Int. J. Fatigue 22, 65–73. https://doi.org/10.1016/S0142-1123(99)00088-2

Lammens, N., Kersemans, M., De Baere, I., Van Paepegem, W., 2017. On the visco-elasto-plastic response of additively manufactured polyamide-12 (PA-12) through selective laser sintering. Polym. Test. 57, 149–155. https://doi.org/10.1016/j.polymertesting.2016.11.032

Meneghetti, G., Ricotta, M., Atzori, B., 2013. A synthesis of the push-pull fatigue behaviour of plain and notched stainless steel specimens by using the specific heat loss. Fatigue Fract. Eng. Mater. Struct. 36, 1306–1322. https://doi.org/10.1111/ffe.12071

Meneghetti, G., Rigon, D., Gennari, C., 2019. An analysis of defects influence on axial fatigue strength of maraging steel specimens produced by additive manufacturing. Int. J. Fatigue 118, 54–64. https://doi.org/10.1016/j.ijfatigue.2018.08.034

Morales-Planas, S., Minguella-Canela, J., Lluma-Fuentes, J., Travieso-Rodriguez, J.A., García-Granada, A.A., 2018. Multi Jet Fusion PA12 manufacturing parameters for watertightness, strength and tolerances. Materials

(Basel). 11, 1–11. https://doi.org/10.3390/ma11081472
Ngo, T.D., Kashani, A., Imbalzano, G., Nguyen, K.T.Q., Hui, D., 2018. Additive manufacturing (3D printing): A review of materials, methods, applications and challenges. Compos. Part B Eng. 143, 172–196. https://doi.org/10.1016/j.compositesb.2018.02.012
O'Connor, H.J., Dickson, A.N., Dowling, D.P., 2018. Evaluation of the mechanical performance of polymer parts fabricated using a production scale multi jet fusion printing process. Addit. Manuf. 22, 381–387. https://doi.org/10.1016/j.addma.2018.05.035
Plekhov, O., Naimark, O., Semenova, I., Polyakov, A., Valiev, R., 2015. Experimental study of thermodynamic and fatigue properties of submicrocrystalline titanium under high cyclic and gigacyclic fatigue regimes. Proc. Inst. Mech. Eng. Part C J. Mech. Eng. Sci. 229, 1271–1279. https://doi.org/10.1177/0954406214563738
Razavi, S.M.J., Ferro, P., Berto, F., Torgersen, J., 2018. Fatigue strength of blunt V-notched specimens produced by selective laser melting of Ti-6Al-4V. Theor. Appl. Fract. Mech. 97, 376–384. https://doi.org/10.1016/j.tafmec.2017.06.021
Revilla-León, M., Özcan, M., 2019. Additive Manufacturing Technologies Used for Processing Polymers: Current Status and Potential Application in Prosthetic Dentistry. J. Prosthodont. 28, 146–158. https://doi.org/10.1111/jopr.12801
Ricotta, M., Meneghetti, G., Atzori, B., Risitano, G., Risitano, A., 2019. Comparison of Experimental Thermal Methods for the Fatigue Limit Evaluation of a Stainless Steel. Metals (Basel). 9, 677. https://doi.org/10.3390/met9060677
Rigon, D., Ricotta, M., Meneghetti, G., 2019. Analysis of dissipated energy and temperature fields at severe notches of AISI 304L stainless steel specimens. Frat. ed Integrita Strutt. 13, 334–347. https://doi.org/10.3221/IGF-ESIS.47.25
Risitano, A., Risitano, G., 2013. Determining fatigue limits with thermal analysis of static traction tests. Fatigue Fract. Eng. Mater. Struct. 36, 631–639. https://doi.org/10.1111/ffe.12030
Risitano, G., Guglielmino, E., Santonocito, D., 2018. Evaluation of mechanical properties of polyethylene for pipes by energy approach during tensile and fatigue tests. Procedia Struct. Integr. 13, 1663–1669. https://doi.org/10.1016/j.prostr.2018.12.348
Schmitt, M., Mehta, R.M., Kim, I.Y., 2019. Additive manufacturing experimental infill testing and optimization for automotive lightweighting. SAE Tech. Pap. 2019-April, 1–8. https://doi.org/10.4271/2019-01-1275
Singamneni, S., Lv, Y., Hewitt, A., Chalk, R., Thomas, W., Jordison, D., 2019. Additive Manufacturing for the Aircraft Industry : A Review Journal of Aeronautics & Aerospace Additive Manufacturing for the Aircraft Industry : A Review. J. Aeronaut. Aerosp. Eng. 8, 0–13. https://doi.org/10.4172/2329-6542.1000214
Stoia, D.I., Mar, L., Linul, E., 2019. Correlations between Process Parameters and Outcome Properties of Laser-Sintered Polyamide.
Vergani, L., Colombo, C., Libonati, F., 2014. A review of thermographic techniques for damage investigation in composites. Frat. ed Integrita Strutt. https://doi.org/10.3221/IGF-ESIS.27.01
Wang, X., Zhao, L., Fuh, J.Y.H., Lee, H.P., 2019. Effect of porosity on mechanical properties of 3D printed polymers: Experiments and micromechanical modeling based on X-ray computed tomography analysis. Polymers (Basel). 11. https://doi.org/10.3390/polym11071154